Pamukkale Univ Muh Bilim Derg, 24(6), 942-951, 2018

Pamukkale Üniversitesi Mühendislik Bilimleri Dergisi

Pamukkale University Journal of Engineering Sciences

Settlements hazard of soil due to liquefaction along Tabriz Metro line 2

Tabriz Metro 2 hattı boyunca sıvılaşmaya bağlı olarak meydana gelen oturma tehlikesi

Masoumeh GHASEMIAN[1], *Rouzbeh DABIRI*[2*], *Rahim MAHARI*[3]

[1]Department of Engineering Geology, Ahar Branch, Islamic Azad University, Ahar, Iran.
masoumeh81geo@yahoo.com
[2]Department of Civil Engineering, Tabriz Branch, Islamic Azad University, Tabriz, Iran.
rouzbeh_dabiri@iaut.ac.ir
[3]Department of Geology, Tabriz Branch, Islamic Azad University, Tabriz, Iran.
mahari@iaut.ac.ir

Received/Geliş Tarihi: 29.03.2017, Accepted/Kabul Tarihi: 14.10.2017
doi: 10.5505/pajes.2017.10336
* Corresponding author/Yazışılan Yazar
Research Article/Araştırma Makalesi

Abstract

After the occurrence of liquefaction due to earthquake, the settlement of soil layers damage to structures located on the ground or the underground. In the last two decades, different experimental methods were used to determine the rate of volumetric strain (settlement) and maximum shear strain based on field and laboratory test data. The main purpose of the present study is the evaluation of the rate of settlement after the occurrence of liquefaction in soils and study relationship between liquefaction potential index (LPI) and settlement. The results of the standard resistance penetration test along Tabriz Metro Line 2 used to estimate the liquefaction potential of soil layers in 54 boreholes. Then, the value of settlement in soil layers due to liquefaction in both dry and saturated soil layers were evaluated. In continue, LPI was calculated. The results of this study showed that the rate of settlement in saturated soil layers was remarkably higher than the layers above the underground water level and with an increase in the density of the soil layers, the rate of settlement and soil volumetric strain decreased. Also, there is a good adoption between LPI and settlement values in soil layers.

Keywords: Liquefaction, Standard penetration test (SPT), Settlement (volumetric strain), Liquefaction potential index (LPI) , Tabriz Metro line 2

Öz

Deprem nedeniyle sıvılaşma meydana geldignde, zemin katmanlarının çozulmesi içinde bulunan veya yeraltı yapılarına hasar verebilir. Son yirmi yılda, farklı deneysel yöntemler alan ve laboratuar test verilerine dayandirilarak hacimsel gerilme (zemin oturmasi) ve maksimum kayma gerginliğini belirlemek için kullanıldı. Bu çalışmanın temel amacı, zemin sıvılaşmasından sonra zemin oturma oranı oranının değerlendirilmesi ve sıvılaşma potansiyel endeksi (LPI) ile oturma arasındaki çalışma ilişkisinin değerlendirilmesidir. Tabriz Metro 2 Hattı boyunca Standard Penetrasyon testi (SPT) 54 sondaj deliğindeki sonuçlarından zemin katmanlarının sıvılaşma potansiyelini tahmin etmek için kullanıldı. Daha sonra hem kuru hem de doymuş zemin katmanlarında sıvılaştırmaya bağlı olarak zemin katmanlarında oturma oranı hesaplanmıştır. Devamında LPI hesaplanmıştır. Çalışmadan elde edilen sonuçlar gösteriyor ki, doymuş zemin katmanlarindaki oturma oranının, yeraltı su seviyesinin üzerindeki zemin katmanlardan belirgin derecede yüksek olduğunu ve zemin katmanlrinin yoğunluğunun arttığında oturma oranının ve zemin hacimsel gerilimin azaldığını gösterdi. Ayrıca, zemin katmanlarında LPI ve zemin oturma değerleri arasında iyi bir uyum var.

Anahtar kelimeler: Sıvılaşma, Standard penetrasyon testi (SPT), Zemin oturmasi (hacimsel gerilme), Sıvılaşma potansiyel indeksi (LPI), Tabriz Metro 2 hatti

1 Introduction

When saturated sand deposits are subjected to shaking during an earthquake, pore water pressure is known to build up leading to liquefaction or loss of strength. The pore water pressure then starts to dissipate mainly towards the ground surface, accompanied by some volume change of the sand deposits which is manifested on the ground surface as settlement (or volumetric strain). Volumetric strain after liquefaction is influenced not only by the density but more importantly by the maximum shear strain which the sand has undergone during seismic loading. The sandy soil layer is saturated and drainage is limited the condition is prepared of fixed volume situation and the major effect of the seismic shocks is generation of exceed pore water pressure. Therefore, the deposit settlement of saturated sand requires a longer time, varying from a few minutes to a few days, depending on the permeability and compressibility of the soil and the length of the drainage path [1]. The main purpose of this study is to evaluate the rate of settlement in the soil layers along Line 2 of Tabriz Metro and correlation with liquefaction potential index (LPI). In continue, in the following paragraphs discussed and described.

2 Liquefaction and settlement

If saturated loose sandy soil layer is subjected to seismic loading it tends to compression and volumetric reduction in the lack of drainage an increase in pore water pressure is probable. If the pore water pressure in the sand deposit increases due to a continuous seismic loading, its quantity be equal to the total stress. Based on the concept of the effective stress, it can be written:

$$\sigma' = \sigma - u \quad (1)$$

Where the effective stress is σ′ and the total stress is σ and the pore water pressure is u, and, if σ is equal to u, σ ′ is equal to zero. In this condition, the loose sandy layer can lost shear strength. Such a condition is called liquefaction. Liquefaction of saturated loose sand during an earthquake is a damaging factor for buildings, earth dams, retaining walls and etc. The

magnitude of an earthquake and its duration, void ratio, relative density, fines content and soil types, over consolidation ratio and the range of shear stress imposed on the soil are important factors for happening of liquefaction. In recent years, various field methods have been employed to assess this phenomenon. The standard penetrations method (SPT) [2]-[5], Cone penetration method (CPT) [6] and geo-seismic tests by measuring the velocity of the shear wave can be mentioned among field methods [7]-[9]. The tendency of sand to become compressed while under earthquake vibration has been studied and analysed. The soil layer compression appears as settlement on the ground surface. The dry sand above ground water level compression occurs rapidly; typically, the settlement of a sand layer is completed after an earthquake, but the settlement of saturated sand requires a longer time. The settlement occurs when the pore pressure caused by earthquake is dissipated. The required time for settlement depends on the permeability and density of the soil and the length of the drainage course, with the time varying from a few minutes to several days. It is difficult to determine the settlement caused by an earthquake. The errors between 25% and 50% are common in the static settlement prediction and these errors increase in the case of more complicated loading of the earthquake [10]. The rate of the settlement in the sand layers, based on the field test in the two states of the dried layers [11]-[12] and the saturated layers [13]-[19] are evaluated.

In continue, general conditions and the soil layering in the study area and summary of the standard penetration method used for assessing the liquefaction potential is described. Also, the evaluation method of the probable settlement in soil layer above and under ground water level states is mentioned. Finally, the results of the study are explained.

3 Geology and general conditions in study area

3.1 Ground water level

In order to assess the liquefaction potential of the soil layer and the rate of settlement (volumetric strain) value, the geotechnical information of 54 boreholes along of the Tabriz Metro Line 2 collected. The Line 2 of the Tabriz city Metro, having an approximate length of 22 km, starts from the vicinity of the railway in the western part of the city and passes through Qaramalek and Qara-aqaj to the Bazar area in the central parts. The line passes the Daneshsara square, goes under the Mehranroud River, proceeding to the Abbasi Street and Shahid Fahmide Square. It continues from the Shahaid Fahmide Square towards the Baghmishe town and by changing its path, goes to the south east and finishing finally in front of the international Exhibition in Tabriz. This route is on even ground from the beginning to Baghmishe, but encounters ups and downs as it proceeds towards a hilly topography in the east. In the eastern part, the difference between the highest and lowest points along the route is about 140 metres. The position of the route is shown in Figure 1.

The level of the ground water can be considered as one of the main factors in the assessment liquefaction potential of the soils. Along the route level of the ground water level changes, so that in one of the drilled bore holes the water in the Artesian condition had overflowed the surface of the bore hole, while in some of the bore holes waters was not found before a considerable depth. The results of the study show that ground water level changes were not much after being static and the higher level of the ground water related to the spring season. Overall, the depth of the ground water was found to vary from 2 to 30 metres. The balance of the ground water decreased from east to west, showing that the water flow was from east to west, corresponding to the slope of the Tabriz plain. Ground water depth variations in the city of Tabriz are seen in Figure 2. Also, ground water level in the bore holes along path is proposed in Figure 3.

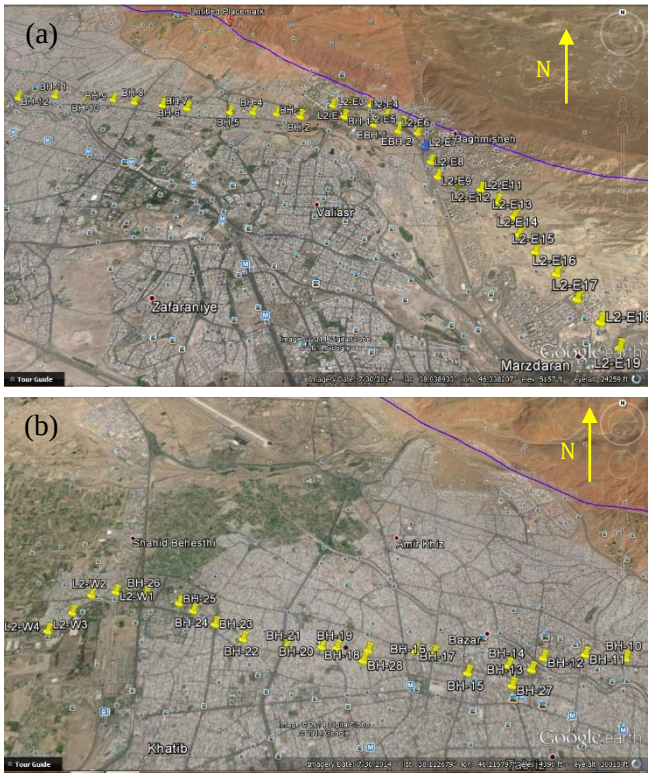


Figure 1: (a),(b): Position boreholes along Tabriz Metro Line 2 [20].

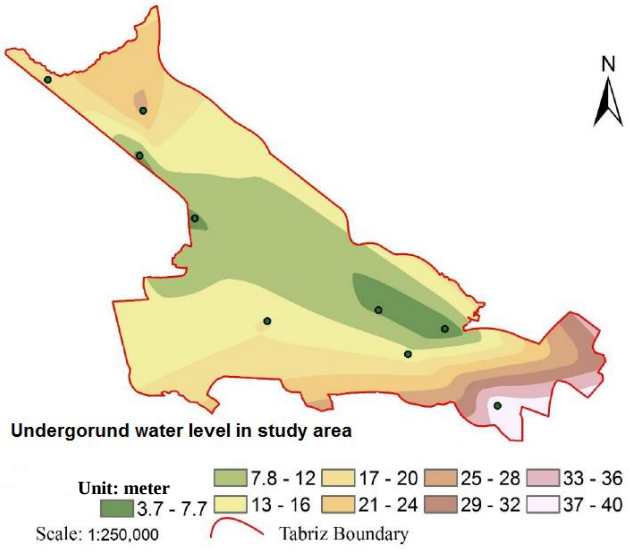


Figure 2: Variation of underground water level in Tabriz city [21].

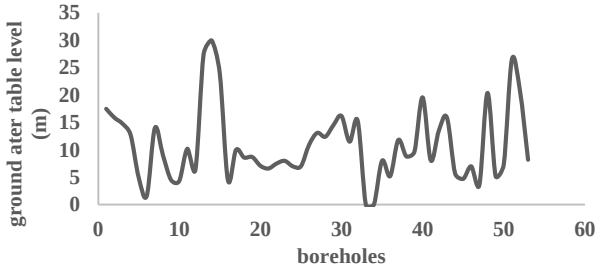


Figure 3: Variation of underground water level in boreholes along Tabriz Metro Line 2.

3.2 General geology of study area

The city of Tabriz is surrounded by the Eynali (Oon-Ebne-Ali) mountain range in the east-west, and not-so-high consolidated alluvial deposits and conglomerates in the south. The general slope of the plain is towards the west and, as a result, the direction of the general drainage of the surface and underground water is also westward. The surface of the plain is generally covered by alluvial deposits. The average height of the city of Tabriz is 1340 metres above sea level. The difference between the highest and the lowest points of Line 2 of the Metro route is 285 metres (Figure 4), [22].

3.3 Soil stratification in study area

Azerbaijan, with respect to stratigraphy, has a long period of expansion and the surroundings of the Tabriz plain also have extensive Cambrian outcrops, but the stones and the alluvium in the area of Tabriz do not date back to such a time period with their formation components being related to the Cenozoic and Quaternary periods. The Cainozoic component in the Tabriz plain started from the Miocene Age and lasted up to the Quaternary era. There is no indication of Palaeocene, Eocene and Oligocene- sediments to indicate pre-Miocene formations, proving that the area is not stratigraphic in nature.

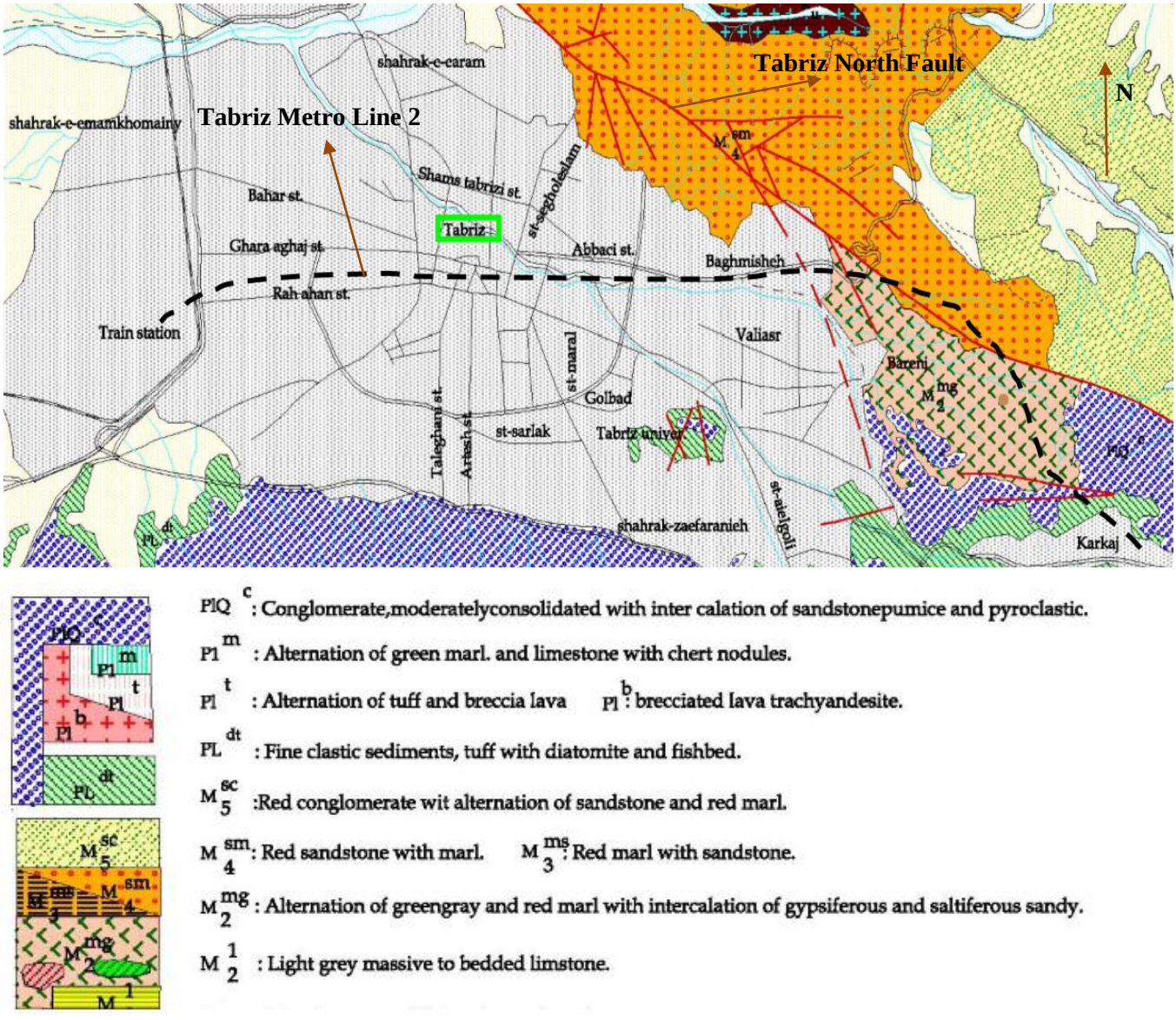


Figure 4: Geology map of Tabriz and Tabriz Metro line 2 (scale 1:100000).

The area under study is inside the city of Tabriz, in the southern part of the mountain range of Eynali that passes through the red Continental classic sediments (mid Miocene) and young alluvial sediment. The red sediments and have gypsum and salt. This formation is mostly composed of sand stone, marl, siltstone and conglomerates along with gypsum and salt. In this area of Tabriz, the continental sediments of Pons in have traces of coal. The mentioned coal is not pure and has been found to be in the form of short and inapplicable shape present in the hills of Baghmishe and Sari Dagh inside the yellow and fossiliferous marl. The marly-hilly formation of Baghmishe that contains coal in the south-west of Tabriz has an outcrop of high thickness, and fish sediment has been located on them at Sinitic, Lapilli and Diatomite. The alluvial of the fourth period including, soft to hard conglomerates, is located on this sediment. The Line 2 of the Tabriz city subway, from its starting point in the west to the Baghmishe town, is covered with alluvial sediment, which , moving west, develops layers of marl and clay stones and siltstone or outcrop comprising a thin covering near the surface of the land. Under the alucia depostes of the Abbasi street towards the east, there are marn and sandstone conglomerate layers at a dept of less than 10 metres. The geological sequances and formations of Tabriz is shown in Table 1.

Table 1: Geological sequances and formations of Tabriz [20].

Quaternary	Alluvium
Pliocene	Fish beds (marl, lapilli, diatomite)
Miocene	Baghmishe formation (marl with shale and lignite) Upper red formation (marl, sandstone, claystone with layer of gypsum)

3.4 Structural geology

The city of Tabriz is located in the west Alborz zone and follows the tectonic regimes ruling it. The forming of the Tabriz plain sediment in it and the formation of tectonic structures that often emerge as fractures or faults follow this system. The Tabriz plain is surrounded in the north by the mountains of Eynali and on the south by the volcanic altitudes of Sahand and its pyroclastic sediments. The reverse function of the north Tabriz Fault with the slope to the north had caused the collapse of its southern part. As a result, parallel to the northern part fractures with normal displacement, the southern plains have been created, resulting in a gardenlike collapse of the east-west continuation. The current formation on which Tabriz is located is the result of such a collapse. As a result of this collapse, the rest of the Miocene and pyroclastic sediment of the east and the south of the city are observable in lower height balances. Furthermore, the erosive function due to the entrance of the big rivers caused the deposit of alluvial material with high thickness in the plain. Regarding the headwaters of the river from the south and the east of the Tabriz plain and its elongation in an east-west state by moving towards the west, particle reduction is expected. According to the fault system activity and the occurred earthquakes in the region and observation of fractures in younger sediments, the area is tectonically active. The Alpine-Himalayan belt is one of the world's most important seismic belts, in which Iran is located. Azerbaijan is also located in this belt and had experienced destructive earthquakes in the past. There are many large and small faults in the region that may cause destructive tremors.

4 Assessment of liquefaction potential

An assessment of the peak ground acceleration (PGA) of study area should be performed to analyze the bore holes and identify the liquefaction potential to determine the rate of settlement in the layers of the soil. The length of Tabriz North fault from Bostan abad to Sofian cities is at least 90 km but it seems to continue towards the south-east and the north-west. Therefore, according to the Iranian Code of Practice for Seismic Resistant Design of Buildings [24] the PGA equal to 0.35g (475 years is the return period and a useful life 50 years) and Mw equal 7.5 are considered. Assessment of the liquefaction potential of the soils in the study area based on the simplified method proposed by Idriss and Bolanger [4] is carried out. In this method, first, the value of cyclic stress ratio (CSR) is estimated expressing the rate of the severity of the earquake load in a Mw=7.5. That is evaluated using the equation bellow:

$$CSR_{7.5} = 0.65.\frac{a_{max}}{g}.\frac{\sigma_V}{\sigma'_V}.r_d.\frac{1}{MSF} \quad (2)$$

Where a_{max} is the peak ground acceleration, g is acceleration of gravity, σ_V total stress in the depth in the question, σ'_V effective stress in the same depth, r_d coefficient of shear stress reduction using the form Figure 5 is estimated and MSF (Magnitude Scale Factor) is earthquake magnitude scale factor that is calculated based on Andrus and stoke researches in 1997 using equation 3. Mw is earthquake magnitude:

$$MSF = \left(\frac{M_W}{7.5}\right)^{-3.3} \quad (3)$$

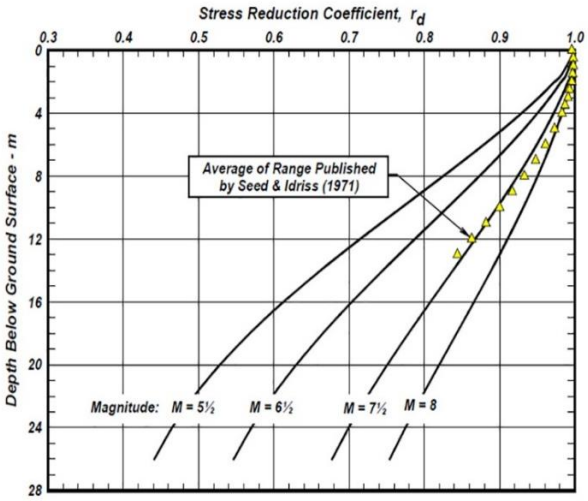


Figure 5: Variations of stress reduction coefficient with depth and earthquake magnitudes [23].

Second, in order to determine to cyclic resistance ratio (CRR) of the soils simplified and modified method proposed by Seed et al. [3] are used. In this step, the results obtained from the standard penetration test are modified based on the following equation proposed by Skempton [25]. Value of parameters can be observed in Table 2.

$$(N_1)_{60} = N_{SPT} \times C_N \times C_E \times C_B \times C_R \times C_S \quad (4)$$

Where, N_{SPT}, the number of standard penetration resistance test, C_N coefficient of the over burden stress, C_E the coefficient

of the hammer energy, C_S the coefficient of the sampling method, C_B the coefficient of the bore hole diameter, C_R the coefficient of the rod length and $(N_1)_{60}$ is the modified number of the standard penetration test. After that, according to the presented proposal by Idriss and Boulanger [4], the overburden tension correction factor (C_N) is determined using the following equation:

$$C_N = (\frac{Pa}{\sigma'_V})^{\alpha} \leq 1.7 \quad (5)$$

$$\alpha = 0.784 - 0.0768 \times \sqrt{(N_1)_{60}} \quad (6)$$

Table 2: Correction factor of SPT [22].

Overburden Pressure		C_N	$(P_a/\sigma'_v)^{0.5}$ $C_N \leq 1.7$
Energy ratio	Donut Hammer Safety Hammer Automatic-Trip Donut-Type Hammer	C_E	0.5 to 1.0 0.7 to 1.2 0.8 to 1.3
Borehole diameter	65 mm to 115 mm 150 mm 200 mm	C_B	1.0 1.05 1.15
Rod length	3 m to 4 m 4 m to 6 m 6 m to 10 m 10 m to 30 m > 30 m	C_R	0.75 0.85 0.95 1.0 ⟨1.0
Sampling method	Standard sampler Sampler without liners	C_S	1.0 1.1 to 1.3

Where, Pa = 100kPa, is the atmospheric pressure and σ'_V is the effective stress at the depth in question, and $(N_1)_{60}$ is corrected the number of standard penetration test. After the modification of the number of the standard penetration test, its equivalent in clean sand ($(N_1)_{60CS}$) is determined. Then, cyclic resistance ratio (CRR) is assessed by the application of the following equations (Figure 6):

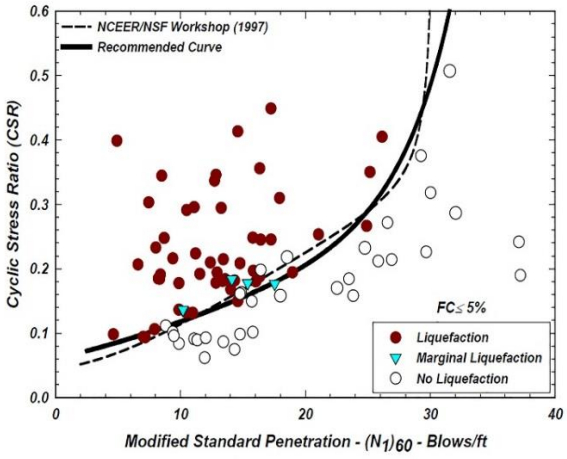


Figure 6: Liquefaction resistance curve for the earthquakes of 7.5 magnitudes [5].

$$(N_1)_{60CS} = (N_1)_{60} + \Delta(N_1)_{60} \quad (7)$$

$$\Delta(N_1)_{60} = 1.63 + \exp\left(1 - \frac{9.7}{FC + 0.1}\right) - (\frac{15.7}{FC + 0.1}) \quad (8)$$

$$CRR = \exp(\left(\frac{(N_1)_{60CS}}{14.1}\right) + \left(\frac{(N_1)_{60CS}}{126}\right)^2 - \left(\frac{(N_1)_{60CS}}{23.6}\right)^3 + \left(\frac{(N_1)_{60CS}}{25.4}\right)^4 - 2.8) \quad (9)$$

Where, FC is equal fines content in soil layer.

In the calculation of the CRR, if the amount of effective vertical stress at the depth in question is more than 100 kPa, the CRR value is modified by using the following equation:

$$CRR_j = K_\sigma \times CRR \quad (10)$$

In this equation, the CRR_j is corrected cyclic resistance ratio. Furthermore, the Kσ parameter is a coefficient based on the effective vertical stress is calculated by the following [26]:

$$K_\sigma = (\frac{\sigma'_V}{100})^{f-1} \quad (11)$$

Where K_σ is the overburden correction factor, σ'_V is the effective vertical stress and f is an exponent that is a function of site conditions including relative density, stress history, aging and over consolidation ratio. For the relative densities between 40% and 60%, f= 0.7-0.8 and for the relative densities between 60% and 80%, f= 0.6-0.7 (Figure 7).

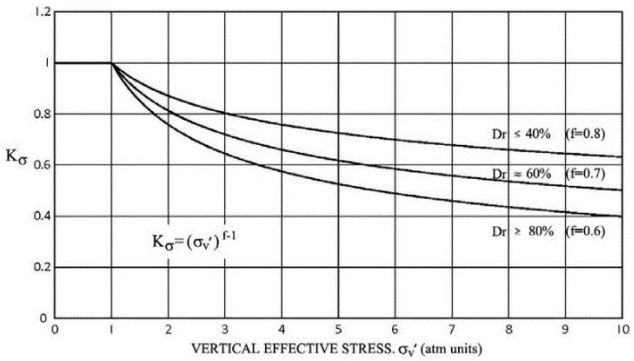


Figure 7: Variations of Kσ values versus effective overburden stress [26].

Safety factor (Fs) against liquefaction in soil layers is calculated using the following equation:

$$F_S = \frac{CRR_j}{CSR} \quad (12)$$

Liquefaction occurs when the amount is Fs ≤ 1; when it is Fs >1 there is no probability of the occurrence of liquefaction.

4.1 Liquefaction potential index (LPI)

The researchers presented several methods for the assessment of the rate of liquefaction and the level of occurrence. One of the common methods is proposed by Iwasaki et al. [27],[28] presented in the following equation:

$$LPI = \int_0^{20} W(Z) \times F(Z).dz \quad (13)$$

$$F(Z) = 1 - F_S \quad \text{For Fs} < 1 \quad (13a)$$

$$F(Z) = 0 \quad \text{For Fs} \geq 1 \quad (13b)$$

$$W(Z) = 10 - 0.5Z \quad \text{For Z < 20 m} \tag{13c}$$

$$W(Z) = 0 \quad \text{For Z > 20 m} \tag{13d}$$

Where, Z is the depth of midpoint in question layer. The Liquefaction intensity is stated between zeros and 100. The liquefaction risk can be obtained using Table 3 based on the liquefaction potential index (LPI) value.

Table 3: Liquefaction potential index (LPI) and its describes [27],[28].

LPI- Value	Liquefaction risk and investigation/Countermeasures needed
LPI=0	Liquefaction risk is very low. Detailed investigation is not generally needed. (very low)
0<LPI≤ 5	Liquefaction risk is low. Further detailed investigation is needed especially for the important structures. (low)
5<LPI≤ 15	Liquefaction risk is high. Further detailed investigation is needed for structures. A countermeasure of liquefaction is generally needed. (high)
LPI> 15	Liquefaction risk is very high. Detailed investigation and countermeasures are needed. (very high)

The liquefaction severity categories proposed by Iwasaki et al. [27],[28] consist of four classes called ‘‘very low,’’ ‘‘low,’’ ‘‘high’’ and ‘‘very high’’ depending on the value of the LPI (Table 3). The areas showing different degree of susceptibility classes and non-susceptible areas may be classified on susceptibility maps such as land slide prone. However, non-susceptible areas could not be distinguished based on the categories proposed by Iwasaki et al.. Furthermore, although ‘‘high’’ and ‘‘low’’ liquefaction potential categories are defined, the category ‘‘moderate’’ is lacking in the categories listed in Table 3. The limitations of the LPI and severity categories (Table 3) were discussed in detail by Sonmez [29] . To overcome these limitations, Sonmez modified F(Z) term appearing the equation of LPI by considering the threshold value of 1.2 between the non-liquefiable and marginally liquefied categories as follow:

$$F(Z) = 0 \quad \text{For} \quad \text{Fs} \geq 1.2 \tag{14a}$$

$$F(Z) = 2 \times 10^6 \times e^{-18.42F_S} \quad \text{For} \quad 0.95 < \text{Fs} < 1.2 \tag{14b}$$

$$F(Z) = 1 - F_S \quad \text{For Fs} < 0.95 \tag{14c}$$

Sonmez introduced two new categories into the classification proposed by Iwasaki et al. [27] as ‘‘non-liquefiable’’ and ‘‘moderate’’ (Table 4). The boundary values of LPI for the categories of ‘‘high’’ and ‘‘very high’’ by Iwasaki et al. preserved by Sonmez. When FL>1.2 throughout the soil column from surface to a depth of 20 m, LPI of the soil column becomes zero and the column is classified as ‘‘non-liquefiable’’ by Sonmez . However, Sonmez pointed out that the threshold value of Fs between non-liquefiable and marginally liquefied conditions (Fs=1.2) is open to discussion, and the threshold value for the non-liquefiable category suggested in his study can be changed depending on the data in future studies. Seed et al. [3] mentioned that the values of Fs against liquefaction ranging between 1.25 and 1.5 are acceptable.

Table 4: Liquefaction potential index (LPI) and its describes [29].

LPI- Value	Liquefaction risk and investigation/Countermeasures needed
LPI=0	Non- Liquefiable (based on Fs ≥ 1.2)
0<LPI≤ 2	Low
2<LPI≤ 5	Moderate
5<LPI≤ 15	High
LPI> 15	Very High

5 Evaluation of settlements in soil layers due to liquefaction

In this study, calculation of the settlement value (volumetric strain) in soil layer after liquefaction have been performed in two sections. The first part is evaluation of the soil layers above the groundwater level and the second part is assessment of the soil layers under the water table. In first part, The Tokimatsu and Seed [15] method have been used for determining the volumetric strain of soil layers above the ground water level in the boreholes (54 boreholes along Tabriz Metro Line 2). The process is described as follows:

1. The relative density (Dr) in soil layers by using the equation No.15 provided by Idriss- Boulanger [4] is determined according for a number of corrected standard penetration resistance test results:

$$D_r = \sqrt{\frac{(N_1)_{60}}{46}} \times 100 \tag{15}$$

2. Assessment of effective shear strain due to earthquake in soil layer with using following relationship that is proposed by Tokimatsu and Seed [4]:

$$\gamma_{eff} = 0.65 \times \frac{a_{max}}{g} \times \frac{\sigma_V}{G_{max}} \times r_d \tag{16}$$

Where, r_d is the stress reduction factor, a_{max} the peak ground acceleration, σ_v represents the total stress at the depth in question, and G_{max} is the maximum shear modulus calculated by below equation that is proposed Tokimatsu and Seed based on kN/m²:

$$G_{max} = 4400 \times ((N_1)_{60})^{0.33} \times (\sigma'_V)^{0.5}) \tag{17}$$

3. After the calculation of the volumetric strain (ε_c) by using the Figure 8 diagrams in each soil layer of boreholes, settlement value in each layer is determined using the following equation:

$$\Delta H = (\frac{\varepsilon_c}{100}) \times h \tag{18}$$

Where, h is the thickness of layer in question. Finally, for each borehole log, the total settlement of soil layers above the groundwater level is accumulated in meter.

Also, the Tokimatsu and Seed [4] method was used in order to determine soil layers settlement at the below of the groundwater level in 54 boreholes of the study area. The procedure is described as follows:

1. The cyclic stress ratio (CSR) due to earthquake in soil layers is estimated with using equation No. 2,
2. Then with using Equation No.7, clean sand equivalent of number standard penetration resistance test ($(N_1)_{60CS}$) for soil layers below the water table is calculated,

3. The volumetric strain value (ε_v) is assessed by determining both the CSR and $(N_1)_{60CS}$ for each soil layers with using the diagrams in Figure 9,
4. Finally, after calculating the volumetric strain (ε_v) in each soil layers, settlement values is determined in meters with using equation No.17 and then total amount of settlement have been calculated.

In final, after summation the amount of settlements in soil layers in the above and below the groundwater level in each boreholes, the total value of settlement calculated.

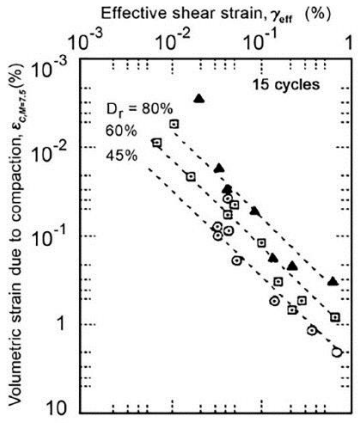


Figure 8: Correlation between volumetric strain and shear strain for Mw=7.5 based on relative density [15].

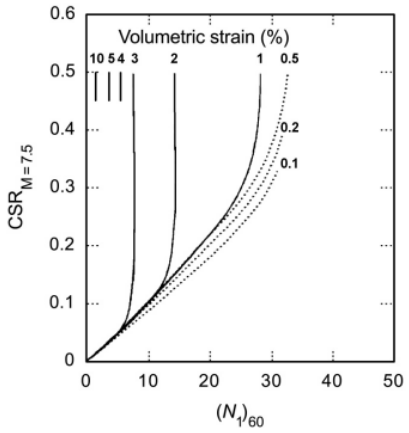


Figure 9: Evaluation of volumetric strain in saturated sand based on CSR and $(N_1)_{60}$ values, Mw=7.5 [15].

6 Results

The results of this study can be explained in below:

1. In 54 of borehole along the Tabriz Metro Line 2, generally the type of the soil layers in 170 samples was sandy, in 213 cases was silty and in 22 cases was gravelly. Moreover, the variation of the number of the standard penetration resistance test results are between 5 and 85. The value of safety factor versus liquefaction in soil layers below ground water level is shown in Figure 10. Accordingly, it can be explained that approximately in 30% to 40% of the data safety factor less than one. This conditions indicant that liquefaction hazard in study area is low to moderate.

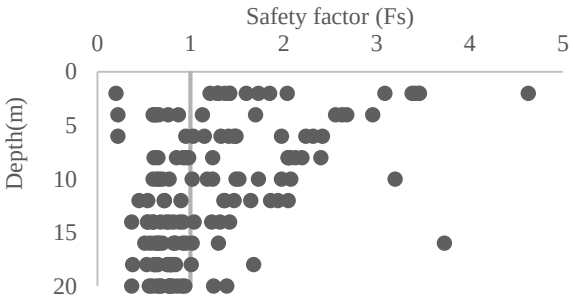


Figure 10: Variation of safety factor against liquefaction versus depth along Tabriz Metro line 2.

2. Effects of fines content and relative density on volumetric strain in soil layers in Mw=7.5 can be illustrated in Figure 11. Accordingly, it is seen with increasing relative density and fines content in soil layers volumetric strain decrease. This result display with reducing void ratio in soil particles and growth fines content settlement hazard due to liquefaction go down.

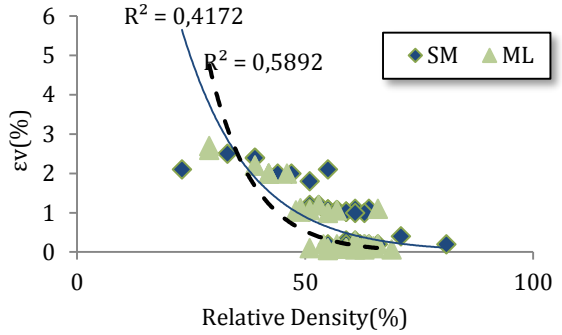


Figure 11: Variations of volumetric strain versus relative density in soil layers (Mw=7.5).

3. Variations of volumetric strain versus effective shear strain (γ_{eff}) due to earthquake in soil layers in Mw=7.5 is observed in Figure 12. As seen on diagrams generally with growing effective shear strain value of volumetric strain trend to rising. But, similarity as mentioned above with increasing fines content volumetric strain declined.

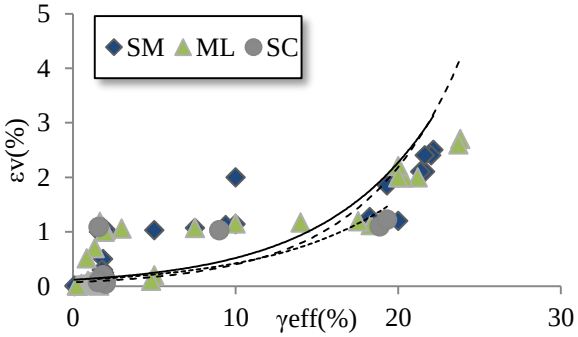


Figure 12: Variations of volumetric strain versus effective shear strain in soil layers (Mw=7.5).

4. The effect of the effective shear strain (γ_{eff}) on volumetric strain (ε_c) in soil layers above ground water level in two section of relative density variations are illustrated in Figures 13 a and b. As can be seen on diagrams, volumetric strain between 40%

to 70% relative densities is more than when relative density grow up to 70%. Also, effects of effective shear strain due to earthquake on volumetric strain in very dense soils is less than moderate dense soils. Although, with increasing fines content in dry soil layers volumetric strain approximately climbed up.

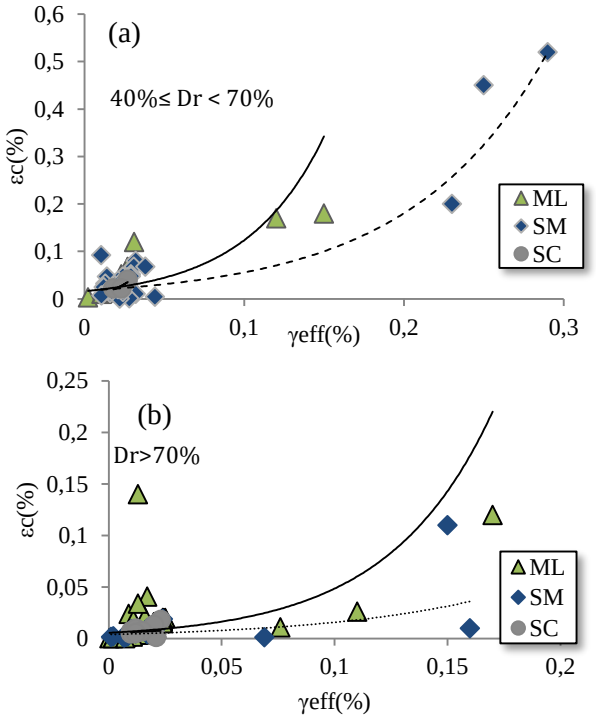


Figure 13: Variations of volumetric strain versus effective shear strain in soil layers above ground water level based relative density a: 40%≤Dr≤70%, b: Dr>70%.

5. Comparison between settlement values of soil layers above and below ground water level can be seen in Figure 14. As shown in diagrams settlement in saturated soil layers due to liquefaction and earthquake is more than dry soils.

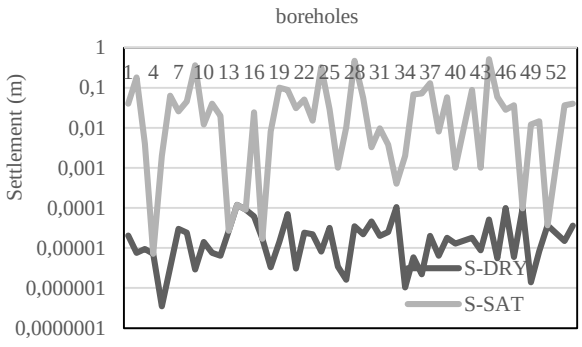


Figure 14: Variations of settlement in dry and saturated soil layer in boreholes in study area.

6. Rate of liquefaction potential index (LPI) along Tabriz Metro Line 2 is observed in Figure 15 and Table 5. Accordingly Iwasaki et al. method, almost 78% of boreholes are included in the range of low to moderate hazard of liquefaction. Also, 22% of boreholes are located in the category of high risk of liquefaction.

Table 5: Values of LPI in boreholes along Tabriz metro line 2.

Liquefaction potential index	LPI=0	0< LPI <5	5< LPI <15	LPI >15
Number	4	14	24	12
Percent (%)	8	26	44	22

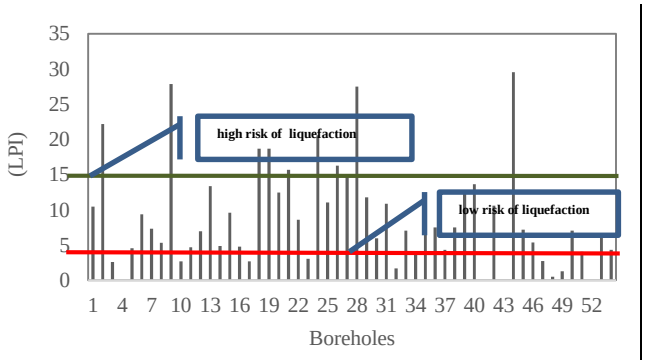


Figure 15: Values of LPI in boreholes in study area.

7. The total settlement values in soil layers of boreholes in study area is illustrated in Figure 16a. Also, variations of LPI is proposed in Figure 16b. With comparison between each other can be seen a suitable correlation. As shown in Figures with increasing in LPI similarity total settlement growth up and vice versa too. Therefore, a range of settlement variations in soil layers in accordance with LPI for study area have been proposed in Table 6. Accordingly, maximum settlement can be happened in along Tabriz Metro Line 2 is more than 9 cm.

Table 6: Values of LPI and total settlement in boreholes along Tabriz metro line 2.

(LPI)	LPI=0	0< LPI <5	5< LPI <15	LPI >15
settlement (m)	HΔ=0	HΔ>0≤0.03	≤0.09 0.03<HΔ	>0.09 HΔ
Number of boreholes	5	16	16	17

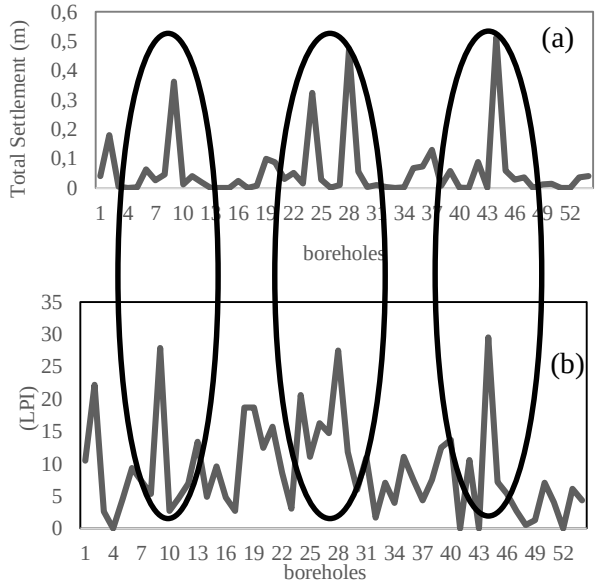


Figure 16: (a): and (b): Comparison of saturated settlement in soil layer and LPI in boreholes in study area.

7 Conclusion and discussion

As mentioned before parts, main goal of this study is evaluation of settlement in soil layers due to liquefaction along Tabriz Metro Line 2. Accordingly, first the liquefaction potential of the layers of soil along the Tabriz Metro Line 2 assessed based on the standard penetration resistance test (SPT) results with using Idriss and Boulanger [4],[5] method. Second LPI determined by Iwasaki et al. [24],[25] procedure and p settlement (volumetric strain) of soil layers due to liquefaction using the Tokimatsu and Seed [15] method. Generally, the results of study showed that:

1. With considering ground water level and type of soils, liquefaction potential in west part of Tabriz (Bazaar to Tabriz Train station) and Metro line 2 is more than east part,
2. Also, there is a good agreement between LPI and total settlement in soil layers due to liquefaction can be seen in west part of Tabriz Metro line 2 the most settlement and volumetric strain values will occur (up to 50 cm),
3. Furthermore, different parameters such as the relative density of the soil, the fines content of soils, the type of fines in soil (clay or silt), the maximum shear strain, and the structure of the grain can affect the value of settlement in soil layers,
4. Therefore, with observing the results suggested that by conducting exact studies through other field tests and analysing them using software more accurate results can be achieved for this field and some methodology proposed for retrofitting critical regions.

8 References

[1] Ishihara K, Yoshimine M. "Evaluation of settlement in sand deposits flowing liquefaction during earthquakes". *Journal of soils and foundations,* 32(1), 173-178, 1992.

[2] Seed H B, Idriss I M. "Simplified procedure for evaluating soil liquefaction potential". *Journal of Soil Mechanics and Foundation Division ASCE*, 97(9), 1249–1273, 1971.

[3] Seed HB, Idriss IM, Arango I." Evaluation of liquefaction potential using field performance data". *Journal of Geotechnical Engineering* (*ASCE*), 1093, 458-482, 1983.

[4] Idriss IM, Boulanger RW. "Semi-empirical procedures for evaluating liquefaction potential during earthquakes". *Soil Dynamic and Earthquake Engineering,* 26, 115-130, 2006.

[5] Idriss IM, Boulanger RW. "SPT-Based Liquefaction Triggering Procedures". Report No. UCD/CGM-10/02, Center for Geotechnical Modeling, University of California, Davis, 2010.

[6] Robertson PK, Wride CE. "Evaluation cyclic liquefaction potential using the cone penetration test". *Canadian Geotechnical Journal,* 35(3), 442-459, 1998.

[7] Andrus RD, Stokoe KH. "Liquefaction Resistance Based on Shear Wave Velocity NCEER Workshop on Evaluation of Liquefaction Resistance of Soils". Technical Report NCEER-97-0022. TL. Youd and IM. Idriss, Eds, Held 4-5 January 1996, Salt lake City, UT, NCEER, Buffalo, NY, 88-128, 1997.

[8] Andrus RD, Piratheepan P, Ellis BS, Zhang J, Juang HC. "Comparing liquefaction evaluation methods using penetration Vs relationship". *Journal of Soil Dynamics and Earthquake Engineering,* 24(2), 713-721, 2004.

[9] Dabiri R, Askari F, Shafiee A, Jafari MK. "Shear wave velocity based Liquefaction resistance of sand-silt mixtures: deterministic versus probabilistic approach". *Iranian journal of science and technology, Transactions of civil engineering,* 35(C2), 199-215, 2011.

[10] Askari F, Dabiri R, Shafiee A, Jafari MK. "Effects of non-plastic fines content on cyclic resistance and post liquefaction of sand-silt mixtures based on shear wave velocity". *Journal of seismology and earthquake engineering,* 12(1, 2), 13-24, 2010.

[11] Pyke R, Seed HB, Chan CK. "Settlement of sands under multidirectional shaking". *Journal of Geotechnical Engineering ASCE*, 101(4), 379 -398, 1975.

[12] Silver ML, Seed HB."Volume changes in sands during cyclic load". *Journal of Soil Mechanics and Foundation Division*, *ASCE*, 97(SM9), 1171-1182, 1971.

[13] Lee KL, Albaisa A. "Earthquake ınduced settlements in saturated sands". *Journal of the Geotechnical Engineering Division ASCE*, 100(4), 387-406, 1974.

[14] Tatsuoka F, Sasaki T, Yamada S. "Settlement in saturated sand ınduced by cyclic undrained simple shear". *8th World Conference on Earthquake Engineering, Sanfrancisco*, 3, 255-262, 1982.

[15] Tokimatsu K, Seed HB."Evaluation of settlements in sand due to earthquake shaking". *Journal of Geotechnical Engineering Division (ASCE)*, 113(8), 861-878, 1987.

[16] Shamato Y, Zhang J, Sato M. "Method for evaluating residual post liquefaction ground settlement and horizontal displacement". *Journal of Soils and Foundations, Special*, 2, 69-83, 1998.

[17] Wu J, Seed RB. "Estimation of liquefaction-ınduced ground settlement (case studies)". *5th International Conference on Case Histories in Geotechnical Engineering, Missouri University of science and Technology*, Missouri, USA, 13-17 April, 2004.

[18] Cetin KO, Unutmaz B. "Probabilistic models for the assessment of post cyclic soil deformations". *9th ASCE Specialty Conference on Probabilistic Mechanics and Structural Reliability*, *Albequerque,* New Mexico, USA, 26-28 July, 2004.

[19] Chen Q, Wang CH, Juang HC. "Probabilistic and spatial assessment of liquefaction-induced settlements through multiscale random field models". *Engineering Geology*, 21(2), 135-149, 2016.

[20] http://google.com/earth/(07/30/2014).

[21] Amiranlou H, Pourkermani M, Dabiri R, Qoreshi M, Buzari S. "Seismic geotechnical micro zonation of tabriz city at veiw of the site affect based on the simulated earthquake". *Open Journal of Earthquake Research,* 5, 114-121, 2016.

[22] Ghobadi MH, Firuzi M, Asghari E. "Relationships between geological formations and ground water chemistry and their effects on concrete lining of tunnels (case study: Tabriz Metro Line 2)". *Environmental Earth Science*, 75(3), 2-14, 2016.

[23] Idriss IM. "An update to the Seed-Idriss simplified procedure for evaluating liquefaction potential". In: Proceedings, TRB workshop on new approaches to liquefaction, publication no. FHWARD-Federal Highway Administration, 99-165, 1999.

[24] Road, housing and urban development research center, "Iran design building against earthquake No. 2800-Version 4". Tehran, Iran, 2014. (In Persian).

[25] Skempton AK. "Standard penetration test procedures and the effects in sands of overburden pressure, relative density, particle size, aging and over consolidation". *Journal of Geotechnique*, 36(3), 425-447, 1986.

[26] Hynes ME, Olsen RS. "Influence of Confining Stress on Liquefaction Resistance". *Proceeding, International Workshop on the Physics and Mechanics of Soil Liquefaction*, *Baltimore, Maryland, U.S.A,* 10-11 September 1998.

[27] Iwasaki T, Tokida K, Tatsuko F, Yasuda S. "A practical method for assessing soil liquefaction potential based on case studies at various sites in Japan". *Proc., 2nd International Conference on Microzonation for safer construction, San Francisco,* November 26-December 1, 1978.

[28] Iwasaki T, Tokida K, Tatsuoka F, Watanabe S, Yasuda S, Sato H. "Microzonation for soil liquefaction potential using simplified methods". *Proc.*, *3rd International Conference on Earthquake Microzonation, Seattle*, Washington, USA, 28 June-1 July , 1982.

[29] Sonmez M, Gokceoglu C. "A liquefaction severity index suggested for engineering practice". *Environmental Geology*, 48(2), 81-91, 2005.